Joined segmentation of nuclei and cells

Gabriel Ravelomanana, Charles Kervrann, Thierry Pécot

Joined segmentation of nuclei and cells

Gabriel Ravelomanana[1], Charles Kervrann[1], Thierry Pécot[2]
[1]SAIRPICO, Inria Center at Rennes University, Rennes, France
[2]FAIIA, Biosit (UAR 3480 CNRS - US 18 Inserm), Rennes University, Rennes, France

Cellpose [1]

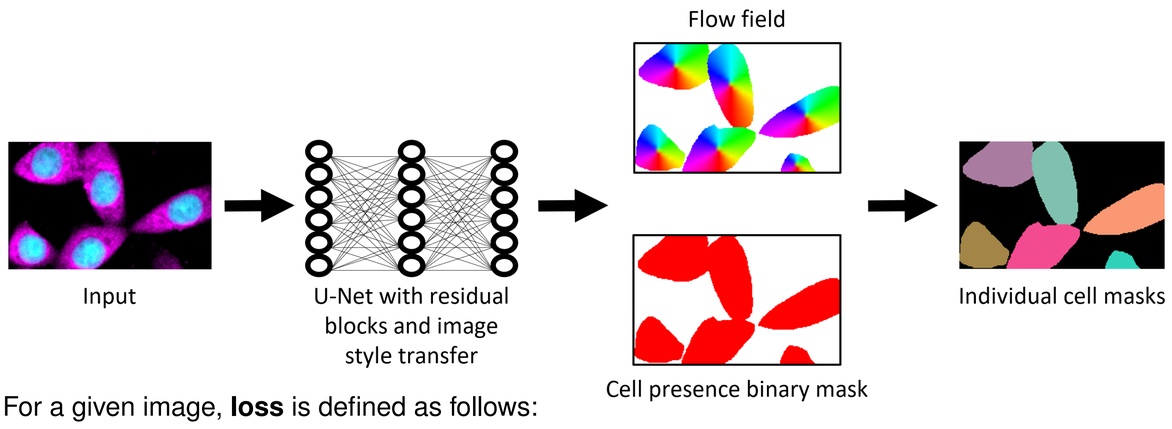

For a given image, **loss** is defined as follows:

- $\mathcal{L}_{cellpose} = \frac{1}{n}\sum_i^n \alpha \underbrace{\|\mathbf{v}_i - \mathbf{v}_i^*\|^2}_{\mathcal{L}_{flow}} - \beta \underbrace{\left((y_i^* \log(y_i) + (1-y_i^*)\log(1-y_i)\right)}_{\mathcal{L}_{CE}}$
  - $\mathbf{v}_i$: predicted flow field at pixel i
  - $\mathbf{v}_i^*$: ground truth flow field at pixel i
  - y_i: predicted cell presence at pixel i
  - y_i^*: ground truth cell presence at pixel i

Evaluation metrics

- $F_1^{0.5} = \frac{2 * TP^{0.5}}{2 * TP^{0.5} + FP^{0.5} + FN^{0.5}}$
  - $TP^{0.5}$: number of true positives for $\tau = 0.5$
  - $FP^{0.5}$: number of false positives for $\tau = 0.5$
  - $FN^{0.5}$: number of false negatives for $\tau = 0.5$
  - τ: Intersection over Union (IoU) threshold
- $F_1^{\mu} = \frac{F_1^{0.5}+F_1^{0.6}+F_1^{0.7}+F_1^{0.8}+F_1^{0.9}}{5}$
- $SQ = \sum_k \mathbb{1}\{IoU_k > 0.5\} IoU_k$, IoU_k: IoU for instance k

Training details

Data	#epochs	Optimizer	l_r	Augmentations
TissueNet [2]	200	Adam	0.005	horizontal/vertical flips, axis-aligned rotations and random crops as in [2, 5]
CPDMI 2023 [3]	1000			

- **2-channel images** for TissueNet [2]
- Input images for TissueNet CPDMI 2023 [3]:
  - **DAPI** channel and **2-4 membranar/cytoplasmic** markers for **training**
  - **average of 7 DAPI** channels and **2 membranar** markers for **test**

Our approach

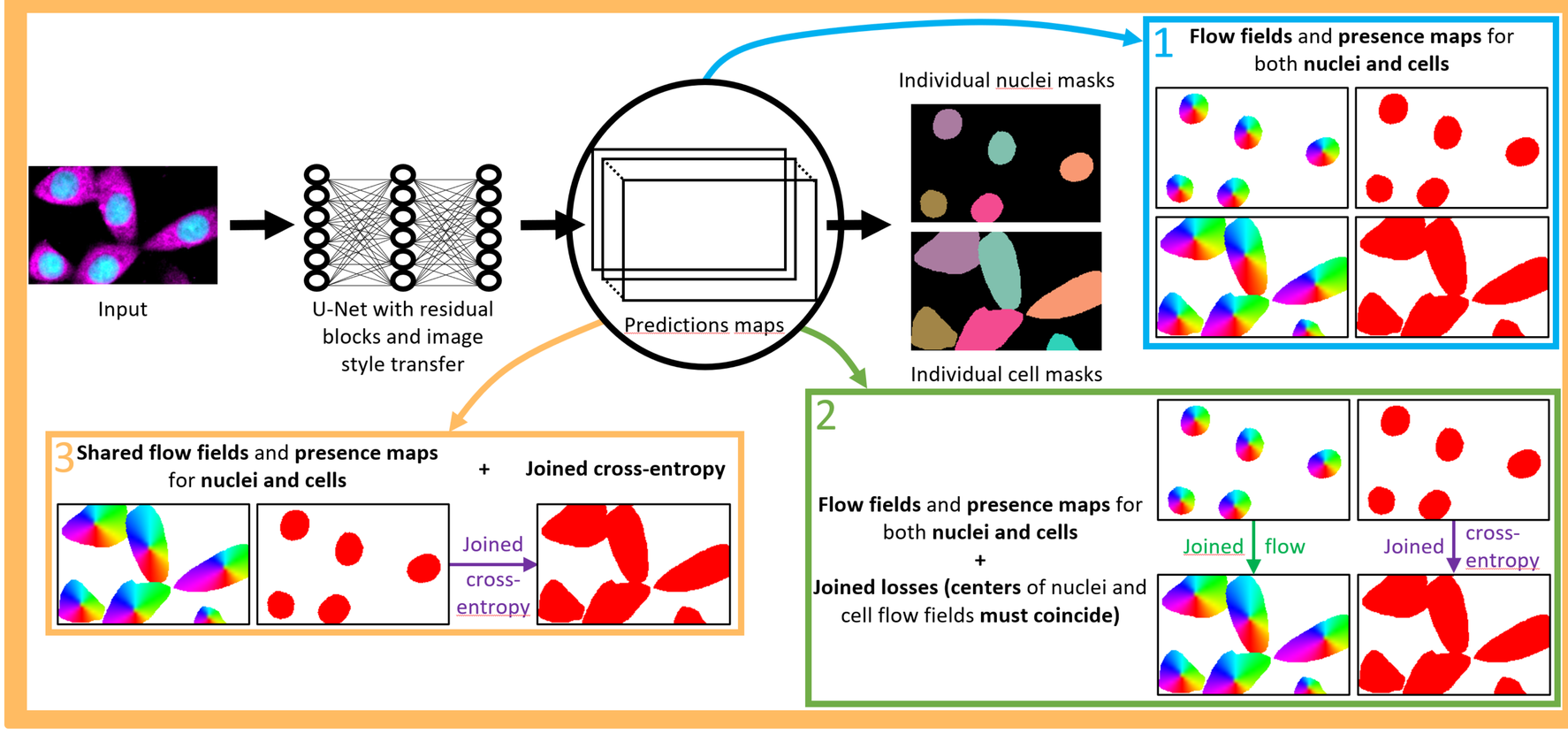

$$\mathcal{L}_1 = \frac{1}{n}\sum_i^n \alpha\left(\underbrace{\|\mathbf{v}_i^n - \mathbf{v}_i^{n*}\|^2}_{\mathcal{L}_{flow}^n} + \underbrace{\|\mathbf{v}_i^c - \mathbf{v}_i^{c*}\|^2}_{\mathcal{L}_{flow}^c}\right) - \beta\underbrace{\left(y_i^{n*}\log(y_i^n) + (1-y_i^{n*})\log(1-y_i^n)\right)}_{\mathcal{L}_{CE}^n} + \underbrace{\left(y_i^{c*}\log(y_i^c) + (1-y_i^{c*})\log(1-y_i^c)\right)}_{\mathcal{L}_{CE}^c}$$

- $\mathbf{v}_i^n$: predicted nuclei flow field at pixel i
- y_i^n: predicted nuclei presence at pixel i
- $\mathbf{v}_i^c$: predicted cell flow field at pixel i
- y_i^c: predicted cell presence at pixel i

$$\mathcal{L}_2 = \mathcal{L}_1 + \frac{1}{n}\sum_i^n \left(\gamma \underbrace{\|\mathbf{v}_i^c \mathbf{v}_i^n\|^2}_{\mathcal{L}_{JF}} - \delta\underbrace{\left(y_i^{n*}\log(y_i^c) + (1-y_i^{n*})\log(1-y_i^c)\right)}_{\mathcal{L}_{JCE}}\right)$$

$$\mathcal{L}_3 = \frac{1}{n}\sum_i^n \alpha\mathcal{L}_{flow} - \beta\left(\mathcal{L}_{CE}^n + \mathcal{L}_{CE}^c\right) - \delta(\mathcal{L}_{JCE})$$

Datasets

TissueNet [2] (7,022 images, 1,343,718 nuclei, 1,428,019 cells)

- **2-channel** images (DAPI/DNA + cytoplasmic/membraner marker)
- **6 modalities**: CODEX, CYCIF, IMC, MIBI, MXIF, VECTRA
- Biopsies from **6 different tissues** (breast, gi, immune, lung, pancreas, skin)
- **Cells** and **nuclei** are annotated for **each image**

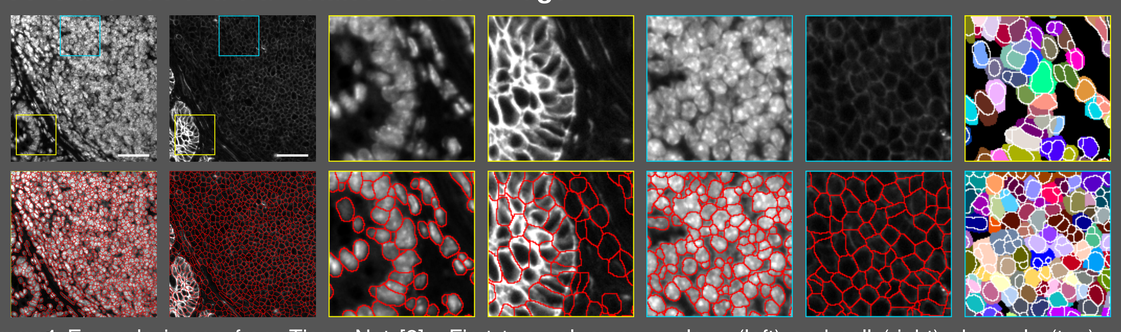

Figure1 Example image from TissueNet [2]. First two columns: nucleus (left) and cell (right) channels (top) with annotated masks overlaid in red (bottom). Scale bars correspond to 50 µm. Next four columns: zoomed-in regions with corresponding squared colors. Last colum: nuclei masks overlaid in white on top of cell masks for zoomed-in regions.

CPDMI 2023 [3] (161 images, 23,663 nuclei, 75,860 cells)

- **multiplexed** images (5 to 32 channels)
- **3 modalities**: Axioscan, CODEX, VECTRA
- Biopsies from **13 different tissues** (lung, breast, pancreas, colon, lymph node, ovary, skin, tongue, sacrum, lymph node, hypopharynx, spleen, tonsil)
- **Cells** and **nuclei** are annotated for **45** images, **only cells** for **113** images and **only nuclei** for **3** images

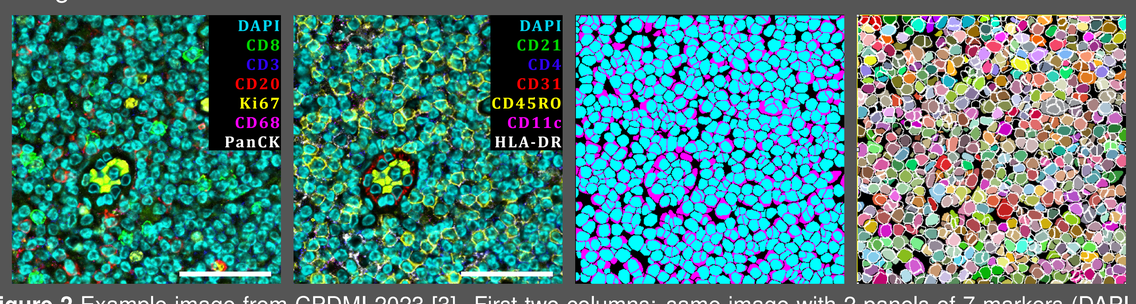

Figure 2 Example image from CPDMI 2023 [3]. First two columns: same image with 2 panels of 7 markers (DAPI is shown in both images). Scale bars correspond to 50 µm. Third column: nuclei masks shown in cyan on top of cell masks shown in magenta. Last colum: nuclei masks overlaid in white on top of cell masks.

	TissueNet [2]			CPDMI 2023 [3]		
	Training	Validation	Test	Training	Validation	Test
#images	2,580	3,118	1,324	131	20	10
#nuclei instances	932,591	275,495	135,633	20,012	2,289	1,362
#cell instances	988,450	294,347	145,222	52,374	17,579	5,907

Results

TissueNet [2]

Method	$F_1^{\mu,n}$	$F_1^{0.5,n}$	SQ^n	$F_1^{\mu,c}$	$F_1^{0.5,c}$	SQ^c	Images / s
*Mesmer [2]	0.7115	0.9030	0.8421	0.6328	0.8593	0.8163	4.7
*InstanSeg [4]	0.7760	0.9160	0.8738	**0.6725**	0.8699	**0.8343**	**42.7**
*InstanSeg + ChannelNet [4, 5]	0.7649	0.9207	0.7646	0.6654	**0.8811**	0.8252	36.8
Cellpose [1]	0.7482	0.8951	0.8458	0.6160	0.8373	0.8024	1.6
$\mathcal{L}_1$	0.8171	**0.9342**	0.8755	0.6604	0.8667	0.8178	3.0
$\mathcal{L}_2$	**0.8195**	0.9308	**0.8767**	0.6513	0.8629	0.8138	2.72
$\mathcal{L}_3$	0.8174	0.9321	0.8758	0.6249	0.8185	0.8203	3.1

First 3 lines with * are reported from [5]

- **Joined training improves** both **nuclei** and **cell** segmentation ($\mathcal{L}_1$ *vs.* Cellpose)
- **Joined flows** do **not improve** segmentation ($\mathcal{L}_2, \mathcal{L}_3$ *vs.* $\mathcal{L}_1$)

Assumption for joined flow failure: **lack of consistency** between **nuclei and cell masks** (Figure 1 last column: several nuclei per cell, several cells per nucleus, discrepancy between cell and nuclei borders) explains the **decrease of performance** for cell segmentation with **joined losses**

CPDMI 2023 [3]

Method	$F_1^{\mu,n}$	$F_1^{0.5,n}$	SQ^n	$F_1^{\mu,c}$	$F_1^{0.5,c}$	SQ^c
*InstanSeg + ChannelNet [4, 5]	0.522	**0.818**	0.767	**0.438**	**0.752**	**0.741**
*InstanSeg - 2 channel (no ChannelNet) [4, 5]	0.498	0.798	0.761	0.380	0.710	0.716
$\mathcal{L}_1$	0.413	0.722	0.735	0.364	0.697	0.709
$\mathcal{L}_2$	0.464	0.773	0.751	0.399	0.740	0.718
$\mathcal{L}_3$	**0.528**	0.804	**0.777**	0.405	0.749	0.719

First 2 lines with * are reported from [5]

- **Joined losses** improve both **nuclei** and **cell** segmentation ($\mathcal{L}_2, \mathcal{L}_3$ *vs.* $\mathcal{L}_1$)
- **Unique** flow field **improves** segmentation ($\mathcal{L}_3$ *vs.* $\mathcal{L}_2$)

While there is **still** a **lack of consistency** between nuclei and cell masks as shown in last column of Figure 2, **joined losses** improve **segmentation performance**

Discussion

- **Joined training improves** both **nuclei** and **cell** segmentation
- **Joined losses** constraining that **cells must exist** where **nuclei lie improve** segmentation
- A **unique flow field** for nuclei and cells **improves** segmentation
- An effort to **enforce annotation consistency** between **nuclei** and **cells might** be **beneficial**
- **Embedding-based segmentation** such as InstanSeg [4] is **much faster** than other DL methods
- **Channel aggregation** strategies like ChannelNet [5] **improves nuclei** and **cell** segmentation

References

[1] Carsen Stringer, Tim Wang, Michalis Michaelos, and Marius Pachitariu, "Cellpose: a generalist algorithm for cellular segmentation," *Nature methods*, vol. 18, no. 1, pp. 100–106, 2021.

[2] Noah F Greenwald, Geneva Miller, Erick Moen, Alex Kong, Adam Kagel, Thomas Dougherty, Christine Camacho Fullaway, Brianna J McIntosh, Ke Xuan Leow, Morgan Sarah Schwartz, et al., "Whole-cell segmentation of tissue images with human-level performance using large-scale data annotation and deep learning," *Nature biotechnology*, vol. 40, no. 4, pp. 555–565, 2022.

[3] Nathaniel Aleynick, Yanyun Li, Yubin Xie, Mianlei Zhang, Andrew Posner, Lev Roshal, Dana Pe'er, Rami S Vanguri, and Travis J Hollmann, "Cross-platform dataset of multiplex fluorescent cellular object image annotations," *Scientific Data*, vol. 10, no. 1, pp. 193, 2023.

[4] Thibaut Goldsborough, Ben Philps, Alan O'Callaghan, Fiona Inglis, Leo Leplat, Andrew Filby, Hakan Bilen, and Peter Bankhead, "Instanseg: an embedding-based instance segmentation algorithm optimized for accurate, efficient and portable cell segmentation," *arXiv preprint arXiv:2408.15954*, 2024.

[5] Thibaut Goldsborough, Alan O'Callaghan, Fiona Inglis, Leo Leplat, Andrew Filby, Hakan Bilen, and Peter Bankhead, "A novel channel invariant architecture for the segmentation of cells and nuclei in multiplexed images using instanseg," *bioRxiv*, pp. 2024–09, 2024.